Michigan State University

National Superconducting Cyclotron Laboratory

ENHANCEMENT OF SYMMETRY VIOLATION IN A CHAOTIC SYSTEM

N. AUERBACH and B. ALEX BROWN

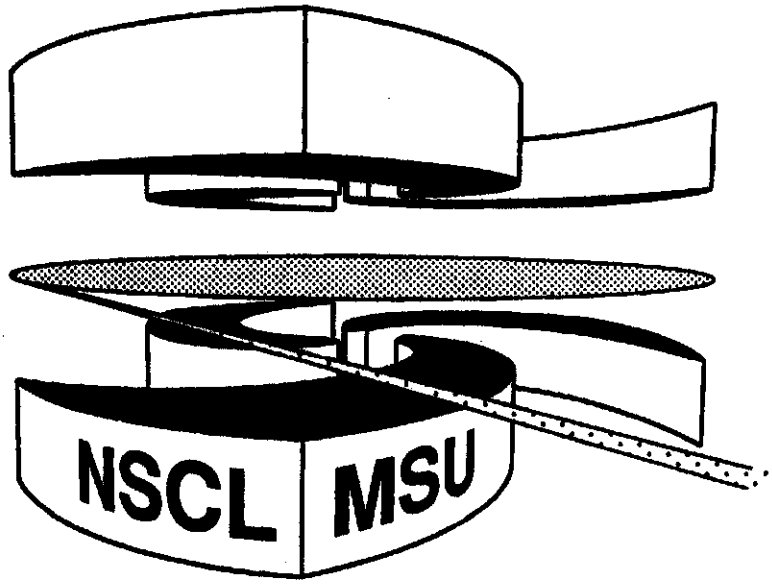

MSUCL-944

AUGUST 1994

Enhancement of Symmetry Violation in a Chaotic System

N. Auarbach

School of Physics and Astronomy
Tel Aviv University,
Tel Aviv 69978, *Israel*

and

B. A. Brown

National Superconducting *Cyclotron* Laboratory
and
Department *of* Physics *and* Astronomy,
Michigan State University,
East Lansing, Michigan *48824-l 321, USA*

Abstract. Enhancement of parity violation effects are calculated in an extended shell model space. Strong enhancements in the longitudinal asymmetry are found when the nucleus is in a regime of large density of states and when nuclear states are very complicated exhibiting features of complete mixing characteristic of the chaotic stage. The nature and mechanism of the enhancement are discussed and compared with parity violation effects found at the single-particle stage. The universality of this effect for a wider class of symmetries and symmetry breakings as well as for a large class of complex systems is mentioned.

It has been conjectured in the past [1, 2], that in the compound nucleus, certain effects of parity and time reversal violation will be enhanced with respect to the same effects when measured for nuclei near their ground state energy. We concentrate on the violation of reflection symmetry and effects of parity mixing in atomic nuclei. When scattering polarized neutrons with helicities $\nu = \pm 1/2$ off unpolarized nuclear targets one can measure the longitudinal asymmetry:

$$P = \frac{\sigma_+(E) - \sigma_-(E)}{\sigma_+(E) + \sigma_-(E)}, \tag{1}$$

where $\sigma_\pm(E)$ are the helicity +1/2 and -1/2 total cross-sections for neutrons with energy E. In the absence of parity violation $P = 0$. A non-zero longitudinal asymmetry signifies the existence of parity non-conservation in the neutron plus target system. The measurements of P are made for p-wave resonances in the compound nucleus. Those p-wave resonances with $J = 1/2^-$ may mix with $J = 1/2^+$ (s-wave) resonances through a parity non-conserving (PNC) force, and therefore give rise to nonzero values for P.

In a number of theoretical works [1, 2, 3, 4, 5] it was shown that the most important term that contributes to P in resonant scattering has the form:

$$P(E_\mu) = 2 \sum_q \frac{< \mu | V_{PNC} | q >}{E_\mu - E_q} \frac{\gamma_q}{\gamma_\mu}, \tag{2}$$

where V_{PNC} is the PNC interaction. The state $|\mu>$ is a $J = 1/2^-$ resonance excited in the reaction and E_μ its energy. The states $|q>$ are $J = 1/2^+$ states

that mix with the resonance $|\mu>$. γ_q and γ_μ are the neutron decay amplitudes to the target ground state of the $|q>$ and $|\mu>$ resonances, respectively. For low neutron energies, due to the centrifugal barrier penetration factor, the ratio for $\ell = 0$ and $\ell = 1$ decays is

$$\frac{\gamma_q}{\gamma_\mu} \simeq \frac{\sqrt{3}}{kR}, \tag{3}$$

where k is the neutron wave number, and R is the nuclear target radius. For $E \simeq 1eV$ and a heavy nucleus this ratio is about 10^3. This enhancement sometimes referred to as "kinematical" is very important in the observation of $P(E_\mu)$ but is not the subject of this paper.

In this work we will be interested in the other quantity in eq.(2), namely in the behavior of:

$$R_{\mu q} = \frac{<\mu|V_{PNC}|q>}{E_\mu - E_q}. \tag{4}$$

It is the behavior of this quantity in the compound nucleus that leads to the "dynamical" enhancement of P in eq.(2).

We may express the decay amplitudes γ_μ and γ_q in the following manner:

$$\gamma_\mu = a_p^{(\mu)} < \varphi_p|U|\chi_p^{(+)}(E_\mu) > \tag{5}$$

and

$$\gamma_q = a_s^{(q)} < \varphi_s|U|\chi_s^{(+)}(E_\mu) >, \tag{6}$$

where φ_p and φ_s are the single-particle bound states, $\chi_p^{(+)}(E)$, $\chi_s^{(+)}(E)$ are the neutron continuum wave functions, and U is a one-body potential. The symbols $a_p^{(\mu)}$ and $a_s^{(q)}$ are the single-particle amplitudes (spectroscopic amplitudes) of the bound p and s states in the wave functions of the $|\mu>$ and $|q>$ states, respectively. Denoting

$$< \varphi_p|U|\chi_p^+(E_\mu) = \gamma_p(E_\mu) \tag{7}$$

$$< \varphi_s|U|\chi_s^+(E_\mu) >= \gamma_s(E_\mu), \tag{8}$$

we write eq.(2) as:

$$P(E_\mu) = 2\frac{\gamma_p(E_\mu)}{\gamma_s(E_\mu)} \sum_q \frac{< \mu|V_{PNC}|q >}{E_\mu - E_q} \frac{a_s^{(q)}}{a_s^{(\mu)}}. \tag{9}$$

In what follows we will mainly deal with the quantity

$$A_\mu = \sum_q \frac{< \mu|V_{PNC}|q >}{E_\mu - E_q} \frac{a_s^{(q)}}{a_p^{(\mu)}}. \tag{10}$$

Let us divide the full parity conserving nuclear Hamiltonian into:

$$H = H_o + V, \tag{11}$$

where H_o represents the mean field Hamiltonian, and V is a residual interaction. We now assume that we are in the energy regime where the nuclear

states $|c>$, which are eigenstates of H when expanded in the basis eigenstates of H_o, will contain a large number - N of "principal" components $|\varphi_i>$; components that all have amplitudes of the same order of magnitude $\frac{1}{\sqrt{N}}$. The number N is proportional to the density of states in the excitation energy regime under discussion. The assumption about the large number of components is an expression of the fact that the nucleus is in a stage of strong mixing; and its wave functions, when expressed in terms of the simple configurations, have amplitudes that are randomly distributed. In this case:

$$|c>=\sum_{i=1}^{N} a_i^{(c)}|\varphi_i> . \tag{12}$$

Let V_{sv} be a one- or two-body interaction that violates a symmetry of H. One can write an off-diagonal matrix element as:

$$<c|V_{sv}|c'>=\sum_{i,j=1}^{N} a_i^{(c)}a_j^{(c')} <\varphi_i|V_{sv}|\varphi_j> . \tag{13}$$

Since the interaction V_{sv} is at most two-body, and in many cases (such as in parity violation in valence orbitals outside of a closed shell) its effective dominant part is one-body, one can connect a given configuration $|\varphi_i>$ to one or very few states $|\varphi_j>$. The double sum in eq. (13) is thus reduced to a single one. For the sake of argument let us write

$$<\varphi_i|V_{sv}|\varphi_j>=p_i\delta_{ij} \tag{14}$$

(for a one-body V_{sv} this is exact in the absence of radial excitations, while

for a two-body V_{sv} there is only a small number of j that will connect to a given i). Then

$$< c|V_{sv}|c' >= \sum_{i=1}^{N} a_i^{(c)} a_i^{(c')} p_i. \tag{15}$$

Because of the "chaotic" nature of the states $|c>$ and $|c'>$ the coefficients $a_i^{(c)}$ are independent random Gaussian variables, and since $\sum_{i=1}^{N} |a_i^{(c)}|^2 = 1$, each $a_i^{(c)}$ is on the average $a_i^{(c)} \simeq \frac{1}{\sqrt{N}}$. From a random walk argument one then obtains

$$\overline{[< c|V_{sv}|c' >^2]}^{1/2} \sim \frac{1}{\sqrt{N}}. \tag{16}$$

The average energy spacing between adjacent levels $|c>$ and $|c'>$ is:

$$E_c - E_{c'} = \frac{\epsilon}{N}, \tag{17}$$

and therefore for such two adjacent levels $|c>$ and $|c'>$

$$\frac{< c|V_{sv}|c' >}{E_c - E_{c'}} \sim \sqrt{N}. \tag{18}$$

We now take V_{sv} to be the PNC interaction V_{PNC}. We obtain for the mixing amplitude

$$\frac{< \mu|V_{PNC}|q >}{E_\mu - E_q} \sim \sqrt{N}. \tag{19}$$

Thus $R_{\mu q}$ is proportional to $\sqrt{N}$ if $|q>$ is a $J = 1/2^+$ level adjacent to the $J = 1/2^-$, $|\mu>$ level. This proportionality to $\sqrt{N}$ is expected to persist in the sum of eq.(2) because the contributions from other terms that come from more distant states $|q>$ will average to zero because of the randomness of sign of the matrix elements and decay amplitudes. Thus only one or very few large terms that stem from levels $|q>$ that are very close to $|\mu>$ will contribute to the sum in eq. (2). For an $E = 1$eV neutron incident on the ^{232}Th target, the excitation energy in the compound ^{233}Th nucleus is $E_x \simeq 4.8$ MeV. At this energy, as already mentioned, the density of states is about 10^5, $J = 1/2$ levels per MeV. When compared to a single-particle spacing this gives $N \simeq 10^6$, and therefore the "dynamical" enhancement is $\sqrt{N} \simeq 10^3$.

In this work we present a numerical study of this enhancement effect. It is impossible to perform a complete calculation of $J = 1/2$ levels in the compound nucleus for a heavy target such as Thorium. We therefore use a light nucleus which should provide a credible model for the situation occurring in heavy mass nucleus. The scale of the spacing between compound levels will be in the keV range rather than eV, but we are able to extrapolate many of our results to the case when the energy spacings are in the eV range.

The calculations were performed for the ^{9}Be nucleus using an extended shell-model space which included the $0s$, $0p$, $1s0d$, and $1p0f$ major oscillator shells. The A=8, $J = 0^+$ ground state was calculated in a $0\hbar\omega + 2\hbar\omega$ model

space which had a matrix dimension of 147. The A=9, $J = 1/2^-$ levels were obtained in a $0\hbar\omega + 2\hbar\omega$ model space, and the $J = 1/2^+$ levels were obtained in a $1\hbar\omega + 3\hbar\omega$ model space. The A=9 matrix dimensions were 647 and 3266, respectively. The parity conserving Hamiltonian was the WBT interaction of Warburton and Brown [6]. In this type of calculation one should take care of the spuriousity introduced by the center-of-mass motion. This was done using the method of Gloeckner and Lawson [7]. We have chosen the excitation energy around $E = 20$ MeV to be the representative energy region, since in nature it involves states that are well described by the theoretical space used here.

The full PNC interaction of DDH [8] was used to calculate the PNC matrix elements between the low-lying states which are predominantly proton (^{9}B) and neutron (^{9}Be) with results of -2.9 eV and 0.6 eV, respectively. Then we introduce an equivalent one-body parity non-conserving (PNC) interaction and compute the matrix elements in which we couple the calculated negative parity $J = 1/2^-$ states to all the computed positive parity $J = 1/2^+$ states. The PNC interaction can be either isoscalar (T=0) or isovector (T=1) and we have used the form:

$$V_{PNC} = \epsilon_T \overrightarrow{\sigma} \cdot \overrightarrow{p}, \tag{20}$$

where $\overrightarrow{\sigma}$ is the nucleon spin, and $\overrightarrow{p}$ is the linear momentum. The coefficients ϵ_T are parameters specifying the strength of the PNC interaction. The values

of ϵ_T were chosen so as to reproduce the above DDH PNC matrix elements in ^{9}B and ^{9}Be.

At this stage we must set the scale by introducing a single-particle estimate for the asymmetry of P in eq.(2). Let $|\mu>$ and $|q>$ be the single-particle $p_{1/2}$ and $s_{1/2}$ states. The value of $E_\mu - E_q$ in this case is determined by the spacings of single-particle states which in the A=9 region is typically

$$\overline{D}_{sp} \equiv E_p - E_s \simeq 15MeV. \tag{21}$$

Since we consider the case of single-particle (sp) states, the ratio of the spectroscopic amplitude $a_s^{(q)}/a_p^{(\mu)}$ is one, and A_μ in eq.(10) is reduced to

$$A_\mu^{sp} = \frac{<\varphi_p|V_{PNC}|\varphi_s>}{E_p - E_s}. \tag{22}$$

Using the above value for $E_p - E_s$ and a value of 3eV for the single-particle PNC element in this mass region, we obtain

$$A_\mu^{sp} \simeq 0.2 \times 10^{-6} \tag{23}$$

This result will serve as a scale in our calculations of A_μ or $R_{\mu q}$.

In Table I we show the r.m.s. of the matrix elements $<\mu|V_{PNC}|q>$ for an ensemble of 21 $J = 1/2^-, |\mu>$ states (state numbers 20-40). Each of these states is coupled to 500 $J = 1/2^+$, $|q>$ states. When taking the average (over the 21, $1/2^-$ states) we obtain

$$\overline{[<\mu|V_{PNC}|q>^2]}^{1/2} \simeq 0.4eV. \tag{24}$$

The average spacing between adjacent levels turns out in our calculation to be

$$\overline{D}_\mu \simeq 150keV. \tag{25}$$

When comparing this spacing to the single-particle spacing of 15 MeV we see that the expected number of principle components - N should be around $\overline{D}_{sp}/\overline{D} \simeq 100$. The r.m.s. PNC matrix element should be reduced by a factor $\sqrt{N} \simeq 10$, compared to the single-particle one, which indeed is the case. We define:

$$R_\mu = \sum_q R_{\mu q} \tag{26}$$

The values of R_μ for the 21 $|\mu>$ states are given in Table I. The q sum is taken in principle over all $J = 1/2^+$ states, but in practice is found to converge for the lowest 500. We see that all the values obtained are larger than the single-particle value in eq. (23). The enhancement factor is on the average around 15, of the same order as $\sqrt{N}$.

In Fig.1 we show the behavior of R_μ as a function of the energy $E_\tau = E_\mu - E_q$. We see that for each $|\mu>$ state the value of R_μ is determined almost completely by the contribution of a few states $|q>$ lying in the immediate vicinity of the state $|\mu>$. The contributions of the more distant states are

reduced in size because of the denominator and mostly cancel out because of the random sign distribution. The amplitudes $a_s^{(q)}$ are also random variables and we should expect similar behavior for the A_μ. Indeed the behavior of A_μ shown in Fig.2 resembles the curves of Fig.1.

We should make the following remark; there are two relevant single-particle p states (the $0p_{1/2}$ and $1p_{1/2}$) that contribute to the spectra we consider. We had to include both when we formed the sum in eq.(8). We did that by replacing $a_p^{(\mu)}$ in the denominator with $a_{0p}^{(\mu)} + a_{1p}^{(\mu)}$. Of course this replacement does not change the behavior of A_μ in Fig.2 for a given μ, but it affects the relative magnitudes of A_μ for different μ. The values of A_μ are given in Table I. Compared to A_μ^{sp}, we find that the enhancement factors fluctuate a lot, but again the average enhancement is around 15. We should also remark that some of the large fluctuation in the value of A_μ are due to the smallness of $a_p^{(\mu)}$ in the denominator. This effect is probably occurring in nature, however we should keep in mind that the $p_{1/2}$ -resonant cross-sections are proportional to $|a_p^{(\mu)}|^2$; and therefore very small values of $a_p^{(\mu)}$ will enhance the asymmetry in eq.(2), but will also at the same time cause the cross-sections to be very small.

One of the important characteristics of symmetry breaking is the symmetry violating spreading width [9, 10, 11]. In the case of PNC the spreading width for a given state $|\mu>$ is:

$$\Gamma^{\downarrow}_{PNC} = \frac{2\pi\overline{<\mu|V_{PNC}|q>^2}}{\overline{D}_{\mu}}, \tag{27}$$

where in the numerator we have the mean square PNC matrix element averaged over the states $|q>$, and $\overline{D}_{\mu}$ is again the average spacing of states $|q>$ in the vicinity of $|\mu>$. In Table I we show the calculated $\Gamma^{\downarrow}_{PNC}$ for 21 states $|\mu>$. The averaging, as before, was performed for 500 states $|q>$ lying in the vicinity of each state $|\mu>$. We see that the values of the spreading widths are fluctuating between $(2-12)\times 10^{-6}eV$ with an average value and variance:

$$\Gamma^{\downarrow}_{PNC} = 7.5 \pm 3.5 \times 10^{-6}eV. \tag{28}$$

In ref. [4] a doorway state model was introduced in which an attempt was made to estimate the PNC spreading width under the assumption that the one-body component of the PNC force is dominating the effects of parity mixing in the compound nucleus. With a one-body PNC force given by eq.(20) the relevant doorway is the giant spin-dipole resonance defined through the collective operator:

$$Q = \sum_i \vec{\sigma_i} \cdot \vec{r_i} \tag{29}$$

We have calculated the distribution of the $\vec{\sigma} \cdot \vec{r}$ (as well as the $\vec{\sigma} \cdot \vec{p}$) strength for the 21 $J = 1/2^-$ states that we analyze. As an example we show in Fig. 3 these two distributions for the $|\mu>$ state number 20. The figure

was drawn so that the strengths (for both $\vec{\sigma} \cdot \vec{p}$ and $\vec{\sigma} \cdot \vec{r}$) are averaged over Gaussians with a width of one MeV. Even though the distributions are fluctuating, one can still see that the strengths for both $\vec{\sigma} \cdot \vec{p}$ and $\vec{\sigma} \cdot \vec{r}$, are similar and exhibit a broad resonance behavior with the center of the resonance lying about 10 MeV above the energy E_μ.

It is worthwhile to make the following remarks. In Fig. 4 we show the distribution of the nearest neighbour level spacings obtained in our calculation and compare it with the Poisson and Wigner distributions. The numerical distribution does not agree with either and its shape is intermediate with respect to the two theoretical shapes. It is customary to refer to the Wigner shape as characteristic of the "chaotic" stage in a quantum system [10]. We see that although the distribution of levels does not reach the fully "chaotic" limit, the "dynamical" enhancement does take place already at an earlier stage.

The "dynamical" enhancement discussed in this paper is not limited to effects of parity violation in compound nuclei. One expects a similar situation to occur for a number of symmetries weakly broken in the nuclear system. Time reversal is an example of such symmetry. Time reversal violation observables that are linearly dependent on the mixing amplitudes will show such effects of enhancement when studied in the compound nucleus regime. Also, "dynamical" enhancement should occur in many complex quantum systems in the situation when the density of states is high and the wave functions

are complicated. Thus enhancement of parity violation should occur also in atoms and molecules.

We wish to thank M. Horoi and V. Zelevinsky for helpful discussions. One of us (N.A.) wishes to thank W. C. Haxton for the hospitality at the Institute of Nuclear Theory where part of this work was performed. We would like to acknowledge support from NSF grant 94-03666. This work was also supported by the US-Israel Binational Science Foundation.

References

[1] R. Haas, L. B. Leipuner and R. K. Adair, Phys. Rev. **116**, 1221 (1959); R. J. Blin-Stoyle, Phys. Rev. **120**, 181 (1960).

[2] O. P. Sushkov and V. V. Flambaum, Sov. Phys. Usp **25**, 1 (1982).

[3] V. E. Bunakov, E. D. Davis and H. A. Weidenmueller, Phys. Rev. C **42**, 1718 (1990).

[4] N. Auerbach, Phys. Rev. C **45**, R514 (1992); N. Auerbach and J. D. Bowman, Phys. Rev. C **46**, 2582 (1992); N. Auerbach and V. Spevak, Phys. Rev. C in press.

[5] J. D. Bowman, G. T. Garvey, C. R. Gould, A. C. Hayes and M. B. Johnson, Phys. Rev. Lett. **68**, 780 (1992).

[6] E. K. Warburton and B. A. Brown, Phys. Rev. C **46**, 923 (1992).

[7] D. H. Gloeckner and R. D. Lawson, Phys. Lett. **53B**, 313 (1974).

[8] B. Desplanques, J. F. Donoghue and B. R. Holstein, Ann. Phys. (N. Y.) **124**, 449 (1980).

[9] J. B. French, V. K. B. Kota, A. Pandey and S. Tomsovic, Ann. Phys. (N. Y.) **181**, 198 (1988).

[10] O. Bohigas and H. A. Weidenmueller, Ann. Rev. Nucl. Part. Sci. **38**, 421 (1988).

[11] N. Auerbach, J. Hufner, A. K. Kerman and C. M. Shakin, Rev. Mod. Phys. **44**, 48 (1972).

Figure Captions:

Fig. 1: R_μ as a function of the maximum energy $E_\tau = E_\mu - E_q$ in the sum of Eq. 26, for state numbers 20 to 29.

Fig. 2: A_μ as a function of E_τ.

Fig. 3: Strength distributions for the matrix elements $\overrightarrow{\sigma} \cdot \overrightarrow{p}$ (dashed line) $\overrightarrow{\sigma} \cdot \overrightarrow{r}$ (solid line) which connects the 20th $1/2^-$ state with all $1/2^+$ states.

Fig. 4: Nearest neighbor level space for the $1/2^-$ and $1/2^+$ states. The spacings for states 20-40 are compared to those expected from the Poission (solid lines) and Wigner (dashed lines) distributions.

Table I: Properties of the PNC matrix elements

state number	$< \mu \vert V_{PNC} \vert q >$ rms (eV)	R_μ (10^{-6})	A_μ (10^{-6})	$\Gamma^{\downarrow}_{PNC}$ (10^{-6} eV)
20	0.51	-6.4	0.5	7.1
21	0.42	-5.8	-3.7	4.8
22	0.45	-5.8	0.7	7.1
23	0.61	4.3	2.7	4.8
24	0.36	-3.3	-0.1	6.1
25	0.37	-1.8	76.4	11.1
26	0.47	6.8	-0.6	3.9
27	0.32	-6.8	-42.0	4.8
28	0.39	-36.9	4.2	7.7
29	0.22	10.9	0.2	3.6
30	0.36	-6.8	-52.9	6.0
31	0.37	4.0	1.1	2.0
32	0.41	20.1	-38.5	6.3
33	0.51	-12.0	36.4	6.6
34	0.43	28.7	-60.6	8.8
35	0.50	4.5	0.7	12.6
36	0.48	-3.6	-2.2	8.9
37	0.44	-4.5	0.2	11.2
38	0.46	33.7	-29.4	10.3
39	0.46	27.3	-5.9	11.1
40	0.31	13.7	-11.3	6.0

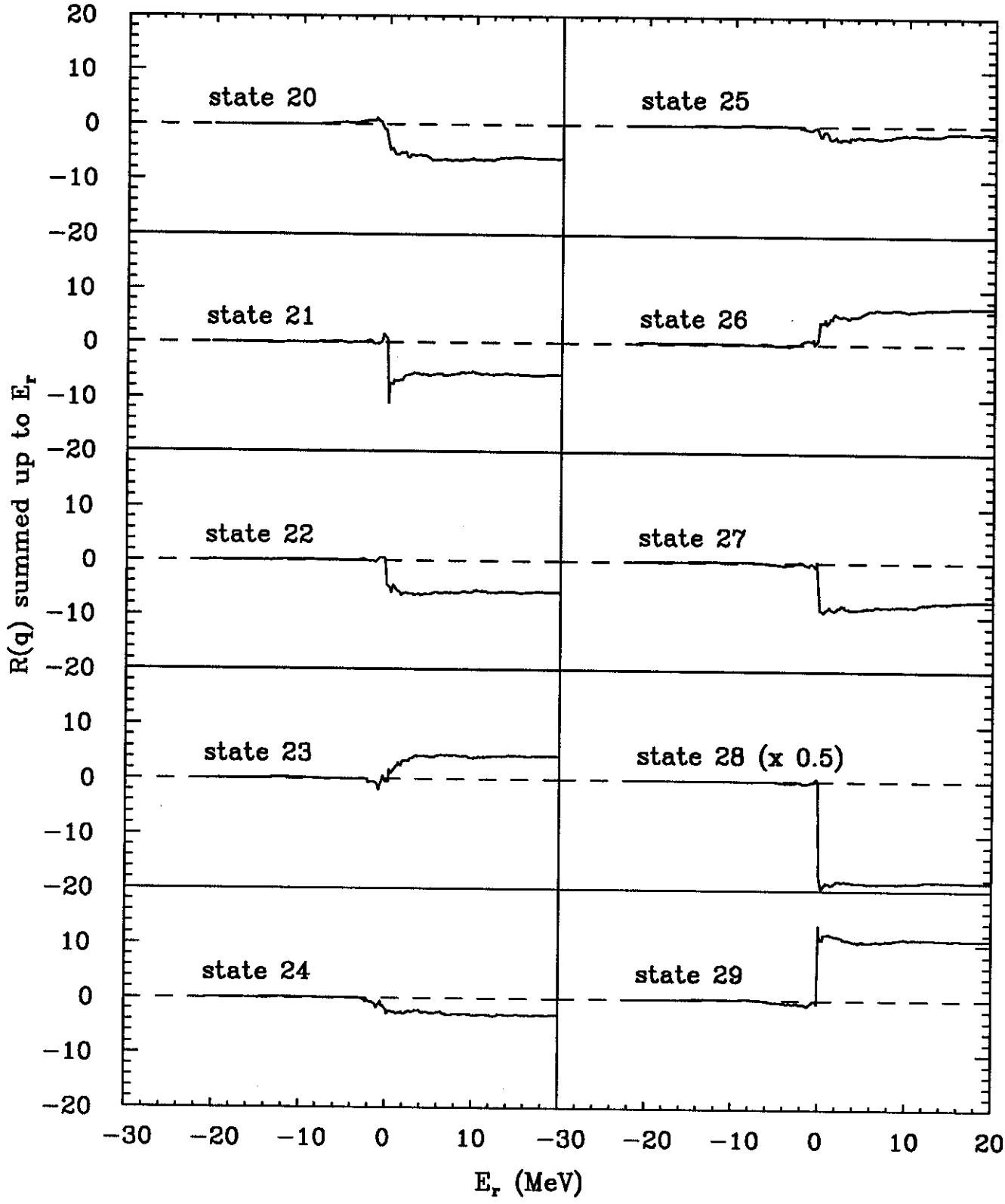
state 20
state 25
state 21
state 26
state 22
state 27
state 23
state 28 (x 0.5)
state 24
state 29
R(q) summed up to E_r
E_r (MeV)
20
10
0
−10
−20
−30

FIGURE 1

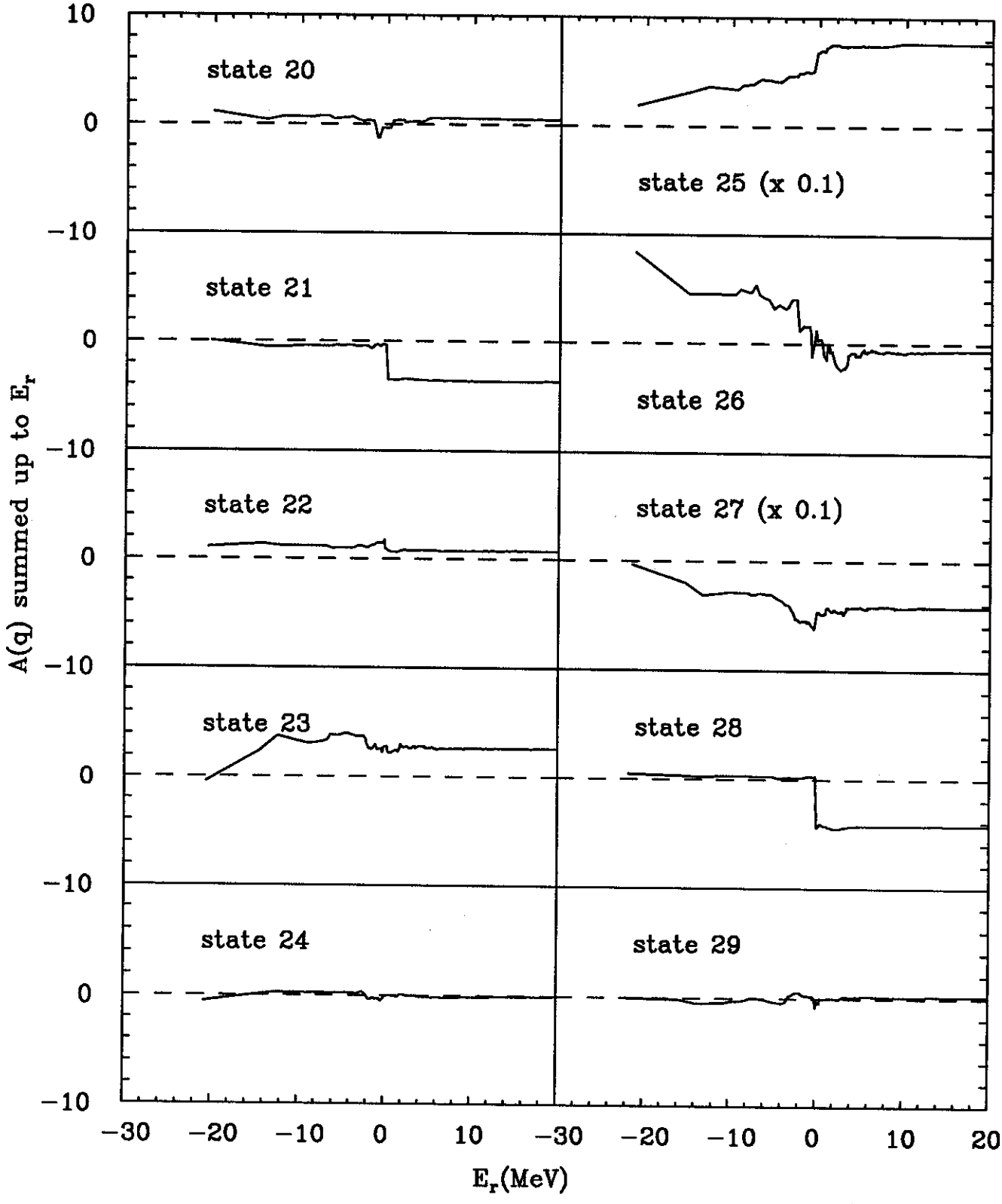
state 20
state 25 (x 0.1)
state 21
state 26
state 22
state 27 (x 0.1)
state 23
state 28
state 24
state 29
A(q) summed up to E_r
E_r(MeV)
10
0
−10
−30
−20
20

FIGURE 2

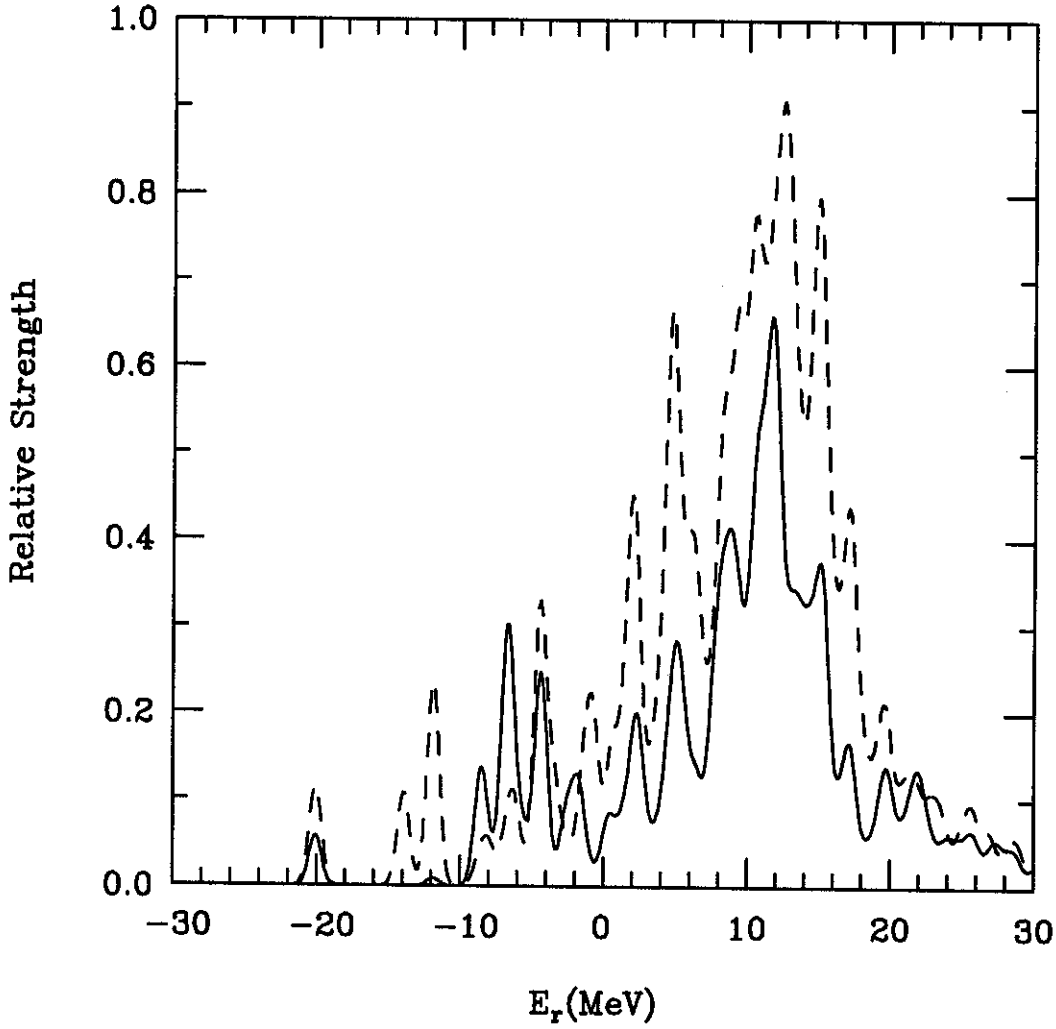

FIGURE 3

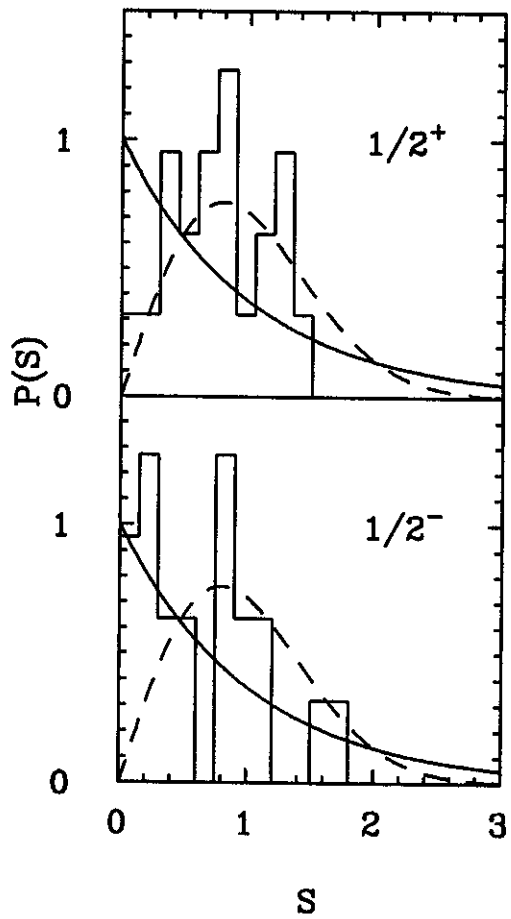

FIGURE 4